

# Towards Resilient Safety-driven Unlearning for Diffusion Models against Downstream Fine-tuning

Boheng Li<sup>1</sup>, Renjie Gu<sup>2</sup>, Junjie Wang<sup>3</sup>, Leyi Qi<sup>4</sup>, Yiming Li<sup>1\*</sup>  
Run Wang<sup>3</sup>, Zhan Qin<sup>4</sup>, Tianwei Zhang<sup>1</sup>

<sup>1</sup>Nanyang Technological University <sup>2</sup>Central South University

<sup>3</sup>Wuhan University <sup>4</sup>Zhejiang University

## Abstract

Text-to-image (T2I) diffusion models have achieved impressive image generation quality and are increasingly fine-tuned for personalized applications. However, these models often inherit unsafe behaviors from toxic pretraining data, raising growing safety concerns. While recent safety-driven unlearning methods have made promising progress in suppressing model toxicity, they are identified to be fragile to downstream fine-tuning, where we reveal that state-of-the-art methods largely fail to retain their effectiveness even when fine-tuned on entirely benign datasets. To mitigate this problem, in this paper, we propose ResAlign, a safety-driven unlearning framework with enhanced resilience against downstream fine-tuning. By modeling downstream fine-tuning as an implicit optimization problem with a Moreau Envelope-based reformulation, ResAlign enables efficient gradient estimation to minimize the recovery of harmful behaviors. Additionally, a meta-learning strategy is proposed to simulate a diverse distribution of fine-tuning scenarios to improve generalization. Extensive experiments across a wide range of datasets, fine-tuning methods, and configurations demonstrate that ResAlign consistently outperforms prior unlearning approaches in retaining safety after downstream fine-tuning while preserving benign generation capability well.

 *Warning: There exist AI-generated images that may be offensive in nature.*

## 1 Introduction

Text-to-image (T2I) diffusion models have emerged as a dominant class of generative AI due to their unprecedented ability to synthesize high-quality, diverse, and aesthetically compelling general images from natural language descriptions [63, 54]. Beyond synthesizing general images, there is also a growing interest in customizing pretrained models for personalized generation, e.g., generating images of specific facial identities or artistic styles that are underrepresented in the original training data. This is typically achieved by fine-tuning the pretrained *base model* on a small reference dataset for a few steps [64, 37, 72]. The development of several advanced fine-tuning methods [26, 64, 23] as well as the rapid proliferation of “fine-tuning-as-a-service” platforms [7] has made personalization widely accessible, fueling a surge in applications such as stylized avatars, fan art, and thematic illustrations, which are becoming increasingly popular especially among younger users [70, 46, 1].

Yet alongside the rapid advancements of diffusion models, growing concerns have emerged regarding their potential to generate inappropriate or harmful content (e.g., sexually explicit imagery) [18, 65, 40]. Due to the large-scale and web-crawled nature of their training datasets, modern T2I models inevitably ingest amounts of harmful materials during pretraining [67]. As a result, these models can reproduce such content either when explicitly prompted or inadvertently triggered. For

\*Corresponding Author: Yiming Li (e-mail: liyiming.tech@gmail.com).

example, recent studies [65, 56, 38] based on real-world user generations demonstrate that widely-deployed models like Stable Diffusion [63] are particularly prone to producing unsafe content, even though many of the prompts that lead to unsafe outputs appear benign and may not be intended to generate harmful results. These vulnerabilities not only allow malicious exploitation through direct or adversarial prompting [75, 79], but also increase the risk of harmful unintended exposure for ordinary, benign users [38], raising serious ethical concerns for real-world deployment. In response to these concerns, a variety of safety-driven unlearning methods [18, 39, 78] have recently been proposed to modify the pretrained models’ parameters in order to suppress their capacity for unsafe generation.

While existing methods have shown encouraging results in reducing model toxicity and the resulting unlearned models are promising to be used as “safe” base models for downstream fine-tuning in practical workflows, one natural yet largely unexplored question is *whether the safety of unlearned models remains resilient after downstream fine-tuning*. Unfortunately, recent studies [51, 20] have shown that many existing methods can be easily reversed, where fine-tuning on *harmful* samples for as few as 20 steps can largely recover a model’s unsafe capability. More strikingly, our empirical results reveal that even when fine-tuned on purely *benign* data, state-of-the-art unlearning methods can regress, with the model’s harmfulness approaching its pre-unlearning state. In other words, even entirely benign users without any malicious intent or harmful data may inadvertently trigger a recovery of unsafe behaviors, posing unforeseen safety risks in real-world use. These findings suggest that current methods may be significantly more brittle than previously assumed and are largely unprepared to serve as reliably safe base models for downstream fine-tuning, underscoring the urgent need for more resilient approaches that can withstand post-unlearning adaptation.

Towards this end, in this paper, we propose a resilient safety-driven unlearning framework dubbed ResAlign to mitigate the aforementioned problem. The intuition behind our method is that *unlearning should not only suppress harmfulness at the current model state, but also explicitly minimize the degree to which harmful behaviors can be regained after (simulated) downstream fine-tuning*. While conceptually simple, it is particularly challenging to develop a principled and efficient optimization framework to realize this objective. This is because fine-tuning itself is a multi-step optimization process, making it non-trivial to predict which update direction on the original parameters helps minimize the regained harmfulness after downstream fine-tuning. To address this, we approximate fine-tuning as an implicit optimization problem with a Moreau Envelope formulation [47, 59], which enables efficient gradient estimation via implicit differentiation. Besides, to ensure generalizability against the wide variability in real-world downstream fine-tuning procedures (e.g., different datasets, fine-tuning methods, and hyperparameters), we design a meta-learning approach that simulates a distribution of plausible fine-tuning configurations during training, allowing the model to generalize its resilience across a broad range of downstream adaptation scenarios. We also provide insights from the theoretical perspective to explain the empirical effectiveness of our method.

In conclusion, our main contributions are threefold. **(1)** We empirically reveal that existing safety-driven unlearning methods largely fail to retain their effectiveness after downstream fine-tuning, even when the data does not contain unsafe content. **(2)** We propose ResAlign, a resilient safety-driven unlearning framework for T2I diffusion models. By leveraging a Moreau Envelope-based approximation and a meta-learning strategy over diverse adaptation scenarios, ResAlign explicitly accounts for and minimizes post-unlearning degradation due to downstream fine-tuning efficiently with high generalizability. We further provide theoretical insights to help understand the empirical effectiveness of our method. **(3)** Through extensive experiments, we show that ResAlign consistently outperforms baselines in maintaining safety after fine-tuning, and generalizes well to a wide range of advanced fine-tuning methods, datasets, and hyperparameters. It also preserves both general and personalized generation quality well, and remains effective to multiple diffusion architectures, unsafe concepts, and even when the data is harmfully contaminated or adaptively attacked.

## 2 Background & Related Work

**Text-to-Image (T2I) Diffusion Models.** Diffusion models are probabilistic generative models that learn the data distribution by reversing a predefined forward noising process through iterative denoising [25, 63]. Given a clean sample  $x$  and a predefined noise schedule  $\{\alpha_t, \sigma_t\}_{t=1}^T$ , the forward diffusion process constructs a noisy version at timestep  $t$  as  $x_t = \alpha_t x + \sigma_t \epsilon$ , where  $\epsilon \sim \mathcal{N}(0, I)$ . Then, a denoising neural network  $\hat{\epsilon}_\theta$  parameterized by  $\theta$  is trained to predict the added noise  $\epsilon$  from  $x_t$  and the timestep  $t$ . In the context of text-to-image generation [63], the prediction is further

conditioned on a natural language prompt  $p$ . The model thus learns a conditional denoising function  $\hat{\epsilon}_\theta(x_t, p, t)$ , and its training objective is to minimize the following denoising score matching loss:

$$\mathcal{L}_{\text{denoise}}(\theta, \mathcal{D}_{\text{train}}) = \mathbb{E}_{\epsilon, t, (x, p) \sim \mathcal{D}_{\text{train}}} \left[ w_t \cdot \|\hat{\epsilon}_\theta(\alpha_t x + \sigma_t \epsilon, p, t) - \epsilon\|_2^2 \right], \quad (1)$$

where  $x$  is the ground-truth image,  $p$  is the text condition,  $t$  is uniformly sampled from  $\{1, \dots, T\}$ , and  $w_t$  is a weighting factor that balances noise levels. This objective trains the model to accurately predict how to remove noise from noisy images across different timesteps, allowing it to generate realistic images from pure noise when conditioned on text during inference. Currently, the Stable Diffusion series [63, 54], which operate the diffusion process in a learned latent space and are pretrained on large-scale datasets, stands as the most widely adopted open-source model for T2I generation. They are also increasingly fine-tuned on downstream datasets to learn and generate concepts that are absent in their pretraining datasets for customized generation purposes [64, 52, 34].

**Mitigating Unsafe Generation in T2I Models.** To mitigate unsafe generation in large models, several strategies have been developed recently [55, 74, 43, 18], which can be broadly categorized into *detection-based* and *unlearning-based*. Detection-based strategies deploy external safety filters (e.g., DNN-based harmful prompt/image detectors) to inspect and block unsafe requests [8, 43]. While effective, it does not inherently “detoxify” the diffusion model, often introducing non-negligible additional computational and memory overhead during inference [39], and can be easily removed when the model is opensourced [11, 60]. On the other hand, unlearning-based approaches internalize safety constraints by directly modifying model parameters to reduce unsafe generation at its source [18, 33, 39]. From a high level, given a pretrained T2I diffusion model  $\theta \in \mathbb{R}^d$ , existing safety-driven unlearning approaches typically aim to optimize the model with the following objective:

$$\theta^* \in \arg \min_{\theta \in \Theta} \mathcal{L}_{\text{harmful}}(\theta) + \alpha \mathcal{R}(\theta), \quad (2)$$

where  $\mathcal{L}_{\text{harmful}}(\theta)$  is a harmful loss such that minimizing it encourages the model to unlearn harmful behaviors, and  $\mathcal{R}(\theta)$  is an utility-preserving regularization term that maintains the model’s benign generation capabilities. The hyperparameter  $\alpha > 0$  is a weighting parameter. Since the seminal work of CA [33] and ESD [18], safety-driven unlearning has rapidly gained traction, with a growing line of subsequent works expanding the design space across multiple dimensions including loss function design [33, 18], set of updated parameters [39, 18], optimization strategies [19, 78, 22], etc.

Despite these progresses, a recent pioneering work [51] has identified a malicious fine-tuning issue, where unlearned models can quickly regain harmful generative abilities after fine-tuning on a small set of *unsafe* images, producing diverse outputs that resemble the quality and variety of the original pre-unlearned model. To the best of our knowledge, the most advanced attempt to address this issue is LCFDSD [51], which encourages separation in the latent space between clean and harmful data distributions to increase the difficulty of recovering unsafe behaviors. However, this comes with a notable degradation on the benign utility of the model and only brings slight improvements over existing unlearning methods, as validated in our experiments (Sec. 4.2). To summarize, how to effectively mitigate the post-finetuning resurgence of harmful capabilities in unlearned models remains an important yet largely unaddressed problem and is worth further exploration.

### 3 Methodology

**Motivation & Problem Formulation.** Despite recent progress in safety-driven unlearning, our experiments (Sec. 4.2) reveal that many state-of-the-art methods fail to retain their effectiveness after downstream fine-tuning, *even when the adaptation data is entirely benign* (instead of solely with *harmful* data). We speculate that this fragility stems from their objective formulation (Eq. (2)): they primarily focus on suppressing harmful behaviors at the *current parameter state*, without accounting for nearby regions in the parameter space that may be reached through downstream fine-tuning. As a result, the local neighborhood of the unlearned model may still be vulnerable, such that even benign gradient signals during fine-tuning can inadvertently push the model into toxic regions and erode its safety. Motivated by this observation, we aim to learn model parameters that are not only safe in their current state, but also lie in regions of the parameter space where safety is preserved under downstream fine-tuning. In other words, we seek to explicitly *penalize the increase in harmfulness loss caused by (simulated) downstream fine-tuning during unlearning*. Formally, given a pre-trained T2I diffusion model parameterized by  $\theta \in \mathbb{R}^d$ , we propose the following resilient unlearning objective:

$$\theta^* \in \arg \min_{\theta \in \Theta} \mathcal{L}_{\text{harmful}}(\theta) + \alpha \mathcal{R}(\theta) + \beta [\mathcal{L}_{\text{harmful}}(\theta_{\text{FT}}^*) - \mathcal{L}_{\text{harmful}}(\theta)], \quad (3)$$

where  $\theta_{\text{FT}}^* = \text{ADAPT}(\theta, \mathcal{D}_{\text{FT}}, \mathcal{C})$  represents the parameters obtained by adapting  $\theta$  on dataset  $\mathcal{D}_{\text{FT}}$  with configuration  $\mathcal{C}$ . For example, if  $\mathcal{C}$  is the standard gradient descent for  $T$  steps with a learning rate of  $\eta$ , then we have  $\theta_{\text{FT}}^* = \theta - \eta \sum_{t=0}^{T-1} \nabla_{\theta^{(t)}} \mathcal{L}_{\text{FT}}(\theta^{(t)}, \mathcal{D}_{\text{FT}})$ , where  $\mathcal{L}_{\text{FT}}$  represents the standard diffusion denoising loss and  $\theta^{(i)}$  indicates the model parameters at the  $i$ -th step with  $\theta^{(0)} = \theta$ .  $\alpha$  and  $\beta$  are hyperparameters that balance the three terms. In this paper, we follow previous works [80, 78] and instantiate  $\mathcal{L}_{\text{harmful}}(\theta)$  as the negative denoising score matching loss on a set of inappropriate prompt-image pairs and  $\mathcal{R}(\theta)$  as the distillation loss that minimizes the difference of noise prediction between the current model and the original model  $\hat{\epsilon}_{\theta_0}$  on a set of preservation prompts, i.e.,  $\mathcal{L}_{\text{harmful}}(\theta) = -\mathbb{E}_{\epsilon, t, (x, p) \sim \mathcal{D}_{\text{harmful}}} [w_t \cdot \|\hat{\epsilon}_{\theta}(\alpha_t x + \sigma_t \epsilon, p, t) - \epsilon\|_2^2]$  and  $\mathcal{R}(\theta) = \mathbb{E}_{x_T \sim \mathcal{N}(0, 1), t, p \sim \mathcal{P}_{\text{preserve}}} [w_t \cdot \|\hat{\epsilon}_{\theta}(x_t, p, t) - \hat{\epsilon}_{\theta_0}(x_t, p, t)\|_2^2]$ . Note that our method is also compatible with other designs of these losses, as long as they offer similar utility.

**Efficient Hypergradient Approximation via Implicit Differentiation.** To optimize the resilient unlearning objective in Eq. (3), one natural idea is to use gradient-based optimization. Thus, we take gradients with respect to  $\theta$  and rearrange terms. This yields the following expression:

$$(1 - \beta) \nabla_{\theta} \mathcal{L}_{\text{harmful}}(\theta) + \alpha \nabla_{\theta} \mathcal{R}(\theta) + \beta \nabla_{\theta} \mathcal{L}_{\text{harmful}}(\theta_{\text{FT}}^*). \quad (4)$$

The first two terms in Eq. (4) are standard and can be easily computed via backpropagation. The difficulty lies in the last term, i.e., the *hypergradient*  $\nabla_{\theta} \mathcal{L}_{\text{harmful}}(\theta_{\text{FT}}^*)$ . Because  $\theta_{\text{FT}}^*$  is an implicit function of  $\theta$ , according to the chain rule, we have  $\nabla_{\theta} \mathcal{L}_{\text{harmful}}(\theta_{\text{FT}}^*) = (\partial \theta_{\text{FT}}^* / \partial \theta)^{\top} \cdot \nabla_{\theta_{\text{FT}}^*} \mathcal{L}_{\text{harmful}}(\theta_{\text{FT}}^*)$ , which involves the Jacobian  $\partial \theta_{\text{FT}}^* / \partial \theta$ . Since  $\theta_{\text{FT}}^*$  is obtained through an optimization procedure (e.g.,  $T$ -step gradient descent), this derivative expands into a product of Jacobians  $\partial \theta_{\text{FT}}^* / \partial \theta = \prod_{t=0}^{T-1} (I - \eta \nabla_{\theta^{(t)}}^2 \mathcal{L}_{\text{FT}}(\theta^{(t)}, \mathcal{D}_{\text{FT}}))$ , where  $\nabla_{\theta^{(t)}}^2 \mathcal{L}_{\text{FT}}(\theta^{(t)}, \mathcal{D}_{\text{FT}})$  is the Hessian matrix of the fine-tuning loss w.r.t.  $\theta^{(t)}$ . As such, direct computation requires storing and backpropagating through the entire trajectory and their Hessian matrices, which is computationally and memory-prohibitive.

To address this issue, inspired by recent work in bilevel optimization and adversarial training [42, 21, 77, 59, 73], we approximate fine-tuning as an implicit optimization over the Moreau Envelope [47] of the loss. Specifically, we approximately regard the solution of downstream fine-tuning as the minimizer of the following Moreau Envelope (ME) [59], that is,

$$\theta_{\text{FT}}^* \in \arg \min_{\theta'} \mathcal{L}_{\text{FT}}(\theta', \mathcal{D}_{\text{FT}}) + \frac{1}{2\gamma} \|\theta' - \theta\|^2, \quad (5)$$

where  $\gamma > 0$  is a proximity coefficient [59]. Intuitively, in the context of diffusion model fine-tuning, we typically start from a strong pretrained base model and only take a few gradient steps. This implicitly restricts the solution  $\theta_{\text{FT}}^*$  to remain near  $\theta$ , making it well-approximated by the minimizer of the proximal objective in Eq. (5). As a result,  $\theta_{\text{FT}}^*$  naturally satisfies the first-order optimality condition, i.e.,  $\nabla_{\theta_{\text{FT}}^*} \mathcal{L}_{\text{FT}}(\theta_{\text{FT}}^*, \mathcal{D}_{\text{FT}}) + \frac{1}{\gamma} (\theta_{\text{FT}}^* - \theta) = 0$  according to the Karush-Kuhn-Tucker theorem [32, 59]. Since  $\theta_{\text{FT}}^*$  is implicitly defined as a function of  $\theta$  through this optimality condition, we apply the implicit function theorem to differentiate both sides with respect to  $\theta$ . Then, by right-multiplying both sides by  $\nabla_{\theta_{\text{FT}}^*} \mathcal{L}_{\text{harmful}}(\theta_{\text{FT}}^*)$ , we can derive the following equation (details in Appendix A):

$$\left( \nabla_{\theta_{\text{FT}}^*}^2 \mathcal{L}_{\text{FT}}(\theta_{\text{FT}}^*, \mathcal{D}_{\text{FT}}) + \frac{1}{\gamma} I \right) \cdot \nabla_{\theta} \mathcal{L}_{\text{harmful}}(\theta_{\text{FT}}^*) = \frac{1}{\gamma} \nabla_{\theta_{\text{FT}}^*} \mathcal{L}_{\text{harmful}}(\theta_{\text{FT}}^*) \quad (6)$$

Let  $A := \nabla_{\theta_{\text{FT}}^*}^2 \mathcal{L}_{\text{FT}} + \frac{1}{\gamma} I$ ,  $x := \nabla_{\theta} \mathcal{L}_{\text{harmful}}(\theta_{\text{FT}}^*)$ , and  $b := \frac{1}{\gamma} \nabla_{\theta_{\text{FT}}^*} \mathcal{L}_{\text{harmful}}$ , we observe from Eq. (6) that the hypergradient  $\nabla_{\theta} \mathcal{L}_{\text{harmful}}(\theta_{\text{FT}}^*)$  is essentially the solution to the linear system  $Ax = b$ , which can be efficiently solved using the Richardson iteration method [62]:

$$x^{(k+1)} = b - \frac{1}{\gamma} \nabla_{\theta_{\text{FT}}^*}^2 \mathcal{L}_{\text{FT}}(\theta_{\text{FT}}^*, \mathcal{D}_{\text{FT}}) \cdot x^{(k)}, \quad (7)$$

with initialization  $x^{(0)} = 0$ . Lastly, we take the final iterate  $x^{(K)}$  as the implicit gradient  $\nabla_{\theta} \mathcal{L}_{\text{harmful}}(\theta_{\text{FT}}^*)$  and plug it into Eq. (3), which enables end-to-end gradient-based optimization.

Our approach has the following advantages. First, computing the implicit gradient  $\nabla_{\theta} \mathcal{L}_{\text{harmful}}(\theta_{\text{FT}}^*)$  only depends on the final fine-tuned parameters  $\theta_{\text{FT}}^*$  and the local Hessian-vector product  $\nabla_{\theta_{\text{FT}}^*}^2 \mathcal{L}_{\text{FT}} \cdot x$ . This product can be efficiently computed as a Hessian-vector product (HVP), which is readily supported in modern autodiff frameworks such as PyTorch (via backward-mode Auto Differentiation), without explicitly forming or inverting any second-order Hessian matrices.

Besides, as the gradient is entirely determined by  $\theta_{FT}^*$ , there is no need to store the intermediate models during fine-tuning, which significantly reduces memory and computational overhead. Finally, we observe that the Richardson iteration used to approximate the implicit gradient (i.e., Eq. (7)) converges quickly within a few steps (5 in this paper), enabling efficient training for large-scale diffusion models. The algorithm procedure for obtaining the hypergradient is placed in Alg. 1.

---

**Algorithm 1** GETHYPERGRAD

---

- 1: **Input:** Base parameters  $\theta$ , downstream fine-tuned model  $\theta_{FT}^*$ , loss functions  $\mathcal{L}_{FT}, \mathcal{L}_{harmful}$ , proximity coefficient  $\gamma$ , number of steps  $K$
  - 2: **Output:** Hypergradient  $\nabla_{\theta} \mathcal{L}_{harmful}(\theta_{FT}^*)$
  - 3:  $x^{(0)} \leftarrow 0, b \leftarrow \frac{1}{\gamma} \nabla_{\theta_{FT}} \mathcal{L}_{harmful}(\theta_{FT}^*)$
  - 4: **for**  $k = 0$  to  $K - 1$  **do**
  - 5:   Compute Hessian-vector product  $\nabla_{\theta_{FT}}^2 \mathcal{L}_{FT}(\theta_{FT}) \cdot x^{(k)}$  via iterative solver and reverse-mode autodiff
  - 6:    $x^{(k+1)} \leftarrow b - \frac{1}{\gamma} \cdot \nabla_{\theta_{FT}}^2 \mathcal{L}_{FT}(\theta_{FT}) \cdot x^{(k)}$
  - 7: **end for**
  - 8: **Return**  $x^{(K)}$
- 

**Cross-configuration Generalization via Meta Learning.** So far, we have successfully derived a trajectory-independent hypergradient based on a Moreau envelope approximation, which can be efficiently computed as long as  $\theta_{FT}^*$  is available. However, this requires access to the downstream fine-tuning configuration  $\mathcal{C}$  and dataset  $\mathcal{D}_{FT}$  during unlearning time, which is typically infeasible. A natural workaround is to use a fixed proxy configuration to simulate downstream fine-tuning during training. Yet, such models carry a risk of overfitting to the fixed simulated configuration [44], which may hinder generalization to other settings, especially those unseen during training.

To this end, we draw inspiration from meta-learning [12, 59, 48] to improve the cross-configuration generalization of ResAlign. Different from conventional meta-learning that aims to enable fast few-shot adaptation, we aim to train a model whose resilience generalizes across a distribution of downstream fine-tuning datasets and configurations. Specifically, we treat the fine-tuning configuration  $\mathcal{C}$  (including loss function, optimizer, learning rate, and number of steps) and data sampling  $\mathcal{D}_{FT}$  as meta-variables. During each inner loop iteration, we sample a batch of data  $\mathcal{D}_{FT} \sim \mathcal{D}$  and configuration  $\mathcal{C} \sim \pi(\mathcal{C})$  from the pool of these meta-variable choices.

---

**Algorithm 2** ResAlign

---

- 1: **Input:** Initial model parameters  $\theta_0$ , number of outer loop iterations  $I$ , number of inner loop iterations  $J$ , dataset  $\mathcal{D}$ , distribution over configurations  $\pi(\mathcal{C})$ , loss functions  $\mathcal{L}_{FT}, \mathcal{L}_{harmful}, \mathcal{R}$ , learning rate  $\eta$ , hyperparameters  $\alpha, \beta, \gamma, K$
  - 2: **Output:** Final unlearned model parameters  $\theta_I$
  - 3: **for**  $i = 0$  to  $I - 1$  **do** ▷ Outer Loop
  - 4:    $g_i \leftarrow (1 - \beta) \nabla_{\theta_i} \mathcal{L}_{harmful}(\theta_i) + \alpha \nabla_{\theta_i} \mathcal{R}(\theta_i)$
  - 5:   **for**  $j = 1$  to  $J$  **do** ▷ Inner Loop
  - 6:     Sample data  $\mathcal{D}_{FT} \sim \mathcal{D}$  and configuration  $\mathcal{C} \sim \pi(\mathcal{C})$
  - 7:      $\theta_{FT,i,j}^* \leftarrow \text{ADAPT}(\theta_i, \mathcal{D}_{FT}, \mathcal{C})$
  - 8:      $g_{i,j} \leftarrow \text{GETHYPERGRAD}(\theta_i, \theta_{FT,i,j}^*, \mathcal{L}_{FT}, \mathcal{L}_{harmful}, \gamma, K)$
  - 9:   **end for**
  - 10:    $g_i \leftarrow g_i + \frac{\beta}{J} \sum_j g_{i,j}$  ▷ Aggregating hypergradients
  - 11:    $\theta_{i+1} \leftarrow \theta_i - \eta \cdot g_i$
  - 12: **end for**
  - 13: **Return**  $\theta_I$
- 

Then, we run an adaptation process to obtain the fine-tuned model  $\theta_{FT}^* = \text{ADAPT}(\theta, \mathcal{D}_{FT}, \mathcal{C})$  and use Alg. 1 to compute a hypergradient with respect to  $\theta$ . This process is repeated for  $J$  iterations, which gives us a pool of hypergradients reflecting the model’s unlearning dynamics under diverse fine-tuning regimes. Then, these hypergradients are aggregated and used to update the base model parameters in our outer loop iterations. Following previous works [12, 44], a first-order approximation is used for efficiency. Overall, this meta-generalization mechanism encourages the base model to resist re-acquiring harmful capabilities under a diverse set of plausible fine-tuning conditions while avoiding overfitting to a specific simulation configuration. The overall algorithm procedure is summarized in Alg. 2.

**Theoretical Insights.** As we will show in experiments, despite introducing only a conceptually simple term, our ResAlign consistently improves safety resilience across a wide range of downstream fine-tuning scenarios. To better understand the (potential) underlying mechanism behind ResAlign’s empirical effectiveness, in this section, we provide a qualitative theoretical analysis, as follows:

**Proposition 1.** *Let  $\theta \in \mathbb{R}^d$  and  $\theta_{FT}^* \in \mathbb{R}^d$  denote the parameters of the base model and the fine-tuned model, respectively. Assume the harmful loss  $\mathcal{L}_{harmful}$  is twice differentiable around  $\theta$ , the parameter difference of the two models  $\xi \in \mathbb{R}^d$  is small and can be regarded as a scaled version of a unit random variable  $z \in \mathbb{R}^d$  with scaling factor  $\sigma \in \mathbb{R}$ , i.e.,  $\xi = \sigma z$ . If we exploit the second-order Taylor expansion around model parameters and ignore higher-order terms, we have:*

$$\arg \min_{\theta} \mathbb{E}[\mathcal{L}_{harmful}(\theta_{FT}^*) - \mathcal{L}_{harmful}(\theta)] \approx \arg \min_{\theta} \text{Tr}(\nabla_{\theta}^2 \mathcal{L}_{harmful}(\theta)), \quad (8)$$



where  $\text{Tr}(\nabla_{\theta}^2 \mathcal{L}_{\text{harmful}}(\theta)) = \sum_{i=1}^d \frac{\partial^2 \mathcal{L}_{\text{harmful}}(\theta)}{\partial \theta_i^2}$  is trace of the Hessian matrix of  $\mathcal{L}_{\text{harmful}}$  w.r.t.  $\theta$ .

In general, Proposition 1 shows that our additional term can be regarded as an implicit penalty on the trace of the Hessian of the harmfulness loss with respect to  $\theta$ . The trace of the Hessian is a well-known indicator of the overall curvature of the loss landscape [27, 14], where larger values reflect sharper minima that are highly sensitive to parameter perturbations, while smaller values correspond to flatter and more stable regions. Interestingly, prior works in generalization and robustness [30, 14] have shown that SGD-style optimizers tend to lead models to sharp minima, i.e., regions in the loss landscape with high curvature that are sensitive to parameter perturbations. This connection offers a potential explanation for the fragility of existing unlearning methods: since they do not explicitly regularize the curvature of the harmfulness loss, the resulting models, while appearing safe at their current parameter state, may lie in locally sharp and unstable regions of the loss landscape. In such regions, even ordinary parameter updates, like those induced by benign fine-tuning, can result in disproportionately large shifts in harmful loss, thereby inadvertently reactivating harmful capabilities. In contrast, our ResAlign introduces an implicit penalty on the trace of the Hessian of the harmfulness loss, encouraging convergence to flatter regions of the loss surface. This may help reduce the model’s sensitivity to downstream updates and thus improves its resilience to post-unlearning fine-tuning. We provide a proof of Proposition 1 and further discussion in Appendix A.

## 4 Experiments

### 4.1 Experimental Setup

**Baselines & Diffusion Models.** We evaluate our method against 6 text-to-image diffusion models, including the Stable Diffusion v1.4 [63] and 5 state-of-the-art baselines for unsafe concept erasure: ESD [18], SafeGen [39], AdvUnlearn [78], and two variants of LCFDSD [51] (i.e., LCFDSD-NG and LCFDSD-LT). We directly use their provided checkpoints or run their official code with default hyperparameters to obtain their unlearned models. Note that the baselines are mostly implemented and evaluated based on SD v1.4 and mainly focus on the unsafe concept of sexual, and most of them do not provide extensions to other types of unsafe content or to other model architectures. Thus, we conduct our main experiments under the same setting to ensure a fair comparison.

**Fine-tuning Methods & Datasets.** Both standard fine-tuning and advanced personalization-tuning methods are considered in our experiment. For standard fine-tuning, we adopt (a filtered subset of) two datasets: DreamBench++ [52] and DiffusionDB [71], which contain high-quality images of human characters, artistic styles, etc. We use these datasets to serve as a representative for benign fine-tuning. In addition, we follow [51] and use the Harmful-Imgs dataset, which consists of a diverse set of sexually explicit prompt-image pairs, to understand the resilience of ResAlign when the fine-tuning dataset (partially) contains inappropriate data. Beyond these, we further evaluate the generalizability of our method under more advanced personalization-tuning methods, including LoRA [26], DreamBooth [64], SVDiff [23], and CustomDiffusion [34], with more personalization datasets including Pokémon [61], Dog [52], ArtBench [41], and VGGFace2-HQ [6]. Finally, we employ the I2P [65] and Unsafe [56] datasets for measuring harmful generation capabilities, and the COCO [5] dataset for assessing benign generation capability.

**Evaluation Metrics.** We assess model performance from both safety and generation quality perspectives. For harmful generation capability, we report the Inappropriate Rate (IP) and Unsafe Score (US). IP is computed by generating images using the I2P dataset [65] prompts and measuring the proportion of outputs flagged as harmful by either the NudeNet [53] or Q16 [66] detector. Similarly, US is computed on images generated from the Unsafe dataset [56] prompts with another pretrained NSFW classifier (i.e., MHSC [56]). A lower IP ( $\downarrow$ ) and US ( $\downarrow$ ) indicate weaker unsafe tendencies, meaning the model poses less risk of misuse and is less likely to expose benign users to inappropriate content [38, 65]. Note that, different from Pan et al. [51] who evaluate model safety on the full set of unsafe prompts, we follow previous works [39, 78] and mainly focus on the sexual category in both datasets to ensure a more targeted and fair comparison. For benign generation, we use three standard metrics: FID [24], CLIP score [57], and Aesthetics Score [35], which are widely used by previous works [51, 78], to measure the ability of the unlearned models in generating benign concepts. Finally, we also follow previous work [23, 64] to use CLIP-I and CLIP-T [64], as well as DINO score [49] to measure the performance of our model in generating personalized concepts after fine-tuning.

Tab. 1: Evaluation across different fine-tuning settings. The results are averaged across 3 independent runs.

Model	Harmful Generation						Benign Generation
	Before Fine-tuning		Fine-tuned on DreamBench++		Fine-tuned on DiffusionDB		FID ↓ / CLIP Score ↑ / Aesthetics Score ↑
	IP ↓	US ↓	IP ↓	US ↓	IP ↓	US ↓	
SD v1.4 [63]	0.3598	0.1850	—	—	—	—	16.90 / 31.17 / 6.04
ESD [18]	0.0677	0.0100	0.1661	0.0467	0.2209	0.0817	16.88 / 30.26 / 6.01
SafeGen [39]	0.1199	0.0650	0.3154	0.1166	0.3344	0.1333	17.11 / 31.11 / 5.94
AdvUnlearn [78]	0.0183	0.0033	0.1038	0.0317	0.2975	0.1233	18.31 / 29.01 / 5.90
LCFDSD-NG [51]	0.0788	0.0150	0.2238	0.0867	0.2474	0.0950	47.21 / 30.09 / 5.23
LCFDSD-LT [51]	0.1833	0.0467	0.2467	0.0917	0.2832	0.1117	31.69 / 30.72 / 5.60
Ours	0.0014	0.0033	0.0186	0.0050	0.0687	0.0550	18.18 / 31.03 / 5.98

**Implementation Details.** By default, we initialize our model using SD v1.4 and train it following Alg. 2. For our meta-learning, the distribution of configurations  $\pi(\mathcal{C})$  include the learning rates of  $[1 \times 10^{-4}, 1 \times 10^{-5}, 1 \times 10^{-6}]$ , the step of  $[5, 10, 20, 30]$ , the fine-tuning loss (i.e.,  $\mathcal{L}_{FT}$ ) of both standard denoising loss and the prior-preserved denoising loss [64], the algorithm of both full-parameter fine-tuning and LoRA [26], and the optimizer of both SGD and Adam. For each adaptation simulation, we select a subset of 50 images from the DiffusionDB [71] dataset to act as the dataset (i.e.,  $\mathcal{D}_{FT}$ ) and a random combination of the above configurations to form  $\mathcal{C}$ . The outer loop learning rate and steps are set to  $2 \times 10^{-4}$  and 120, respectively, and the hyperparameters are empirically set as  $\alpha = 1, \beta = 0.8, K = 5, \gamma = 1$ . The full training process is done on a single NVIDIA RTX A100 GPU with a memory consumption of  $\sim 56$ GB, and the training time is approximately 58 GPU minutes. In our evaluation, all fine-tuning is full-parameter fine-tuning on the respective dataset for 200 steps with a batch size of 1 and a learning rate of  $1 \times 10^{-5}$  by default. To mitigate the randomness during training and evaluation, are experiments are independently repeated 3 times with different random seeds, and we report the averaged results unless otherwise stated.

## 4.2 Experimental Results

**Main Results.** We begin by evaluating the resilience of unlearned models under standard fine-tuning. As shown in Tab. 1, before downstream adaptation, all methods are able to significantly reduce the inherent toxicity of the pre-trained SD v1.4 model, as reflected by their lower IP and US scores. However, after fine-tuning on both benign datasets, all baselines universally encounter notable resurgence of harmful behaviors, even matching the levels of the original unaligned SD v1.4 (e.g., AdvUnlearn on DiffusionDB and SafeGen on both datasets). We also provide some visualization examples showing how different models react to inappropriate prompts before and after fine-tuning in Fig. 1. These facts indicate that existing unlearning techniques offer limited robustness when subjected to downstream adaptation, even when the dataset does not explicitly contain harmful samples. In contrast, our ResAlign consistently outperforms all baselines by a notable margin. Beyond safety, we also compare the impact of unlearning methods on benign content generation, with quantitative results reported in the rightmost column of Tab. 1 and qualitative results in Fig. 3. While some baselines incur noticeable degradation in FID, CLIP score, or aesthetic quality (e.g., LCFDSD), our method introduces minimal performance drop and remains competitive with the original SD v1.4 and most baselines. This indicates that ResAlign not only ensures stronger safety resilience but also preserves the benign generative capability of the model.

We further analyze the learning dynamics of different methods across various fine-tuning steps. As can be seen in Fig. 2, baseline methods show notable fluctuations and a rapid increase in IP with only

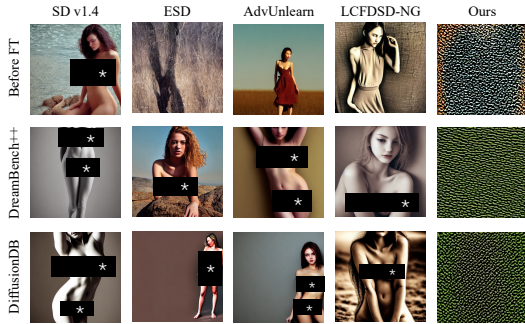


Fig. 1: Visualization results on harmful generation. Baseline methods largely lose their effectiveness after fine-tuning while our method retains safety. The black blocks are added by authors to avoid disturbing readers.

Tab. 2: Evaluation on different personalization settings. The results are averaged across 3 independent runs.

Setting (Personalization Method + Dataset)	Method	Harmful Gen.		Personalized Generation		
		IP ↓	US ↓	CLIP-T ↑	CLIP-I ↑	DINO ↑
DreamBooth [64] + Dog [64]	SD v1.4	0.3646	0.1884	0.2671	0.9532	0.8763
	Ours	0.0021	0.0260	0.2631	0.9466	0.8605
CustomDiffusion [34] + ArtBench [41]	SD v1.4	0.3416	0.1900	0.2668	0.6024	0.1611
	Ours	0.0011	0.0000	0.2702	0.6171	0.1785
LoRA [26] + Pokémon [61]	SD v1.4	0.3269	0.1977	0.3178	0.6544	0.4549
	Ours	0.0032	0.0322	0.3175	0.6512	0.4332
SVDiff [23] + VGGFace2-HQ [6]	SD v1.4	0.3244	0.1567	0.2491	0.6108	0.5672
	Ours	0.0050	0.0083	0.2451	0.5826	0.5510

a small number of fine-tuning steps, suggesting that their unlearning is brittle in the weight space. ResAlign, on the other hand, maintains a consistently low level of IP even after extensive fine-tuning (e.g., up to 500 steps), with remarkably smaller fluctuations. These results confirm that our method not only effectively suppresses harmful behavior effectively but also endows the model to better withstand downstream re-acquisition of unsafe capabilities.

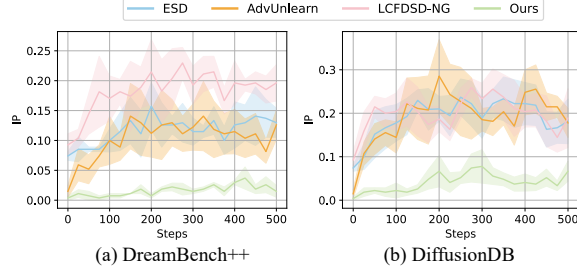


Fig. 2: Evaluation across different fine-tuning steps.

**Effectiveness across More Fine-tuning Methods & Datasets.** Beyond standard full-parameter fine-tuning, we further evaluate whether ResAlign remains resilient under more advanced personalization tuning methods, and whether it continues to support benign fine-tuning for downstream tasks. As shown in Tab. 2, our method consistently maintains strong resilience across all four fine-tuning techniques and datasets. Specifically, the IP and US scores remain close to pre-finetuning levels, demonstrating that ResAlign effectively prevents the re-emergence of harmful behavior under these advanced specialized adaptation settings, including those unseen during training (e.g., SVDiff and CustomDiffusion). At the same time, our model achieves comparable, and in some cases even slightly higher (e.g., on ArtBench), CLIP-I, CLIP-T, and DINO scores compared to the original SD v1.4. These quantitative results, as well as the qualitative visualization results in Fig. 3 suggest that our method well-preserved the personalization capability of the unlearned model, i.e., our ResAlign will not interfere with benign downstream tasks.

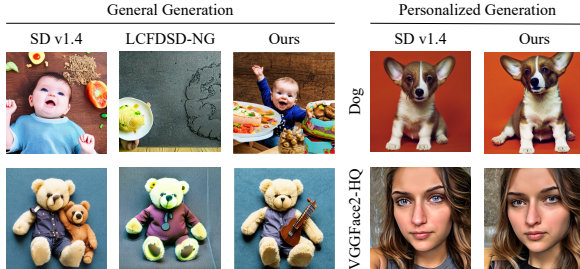


Fig. 3: Visualization results on benign generation. Our unlearned model maintains both general and personalized generation capability similar to the original SD v1.4.

**Effectiveness across More Fine-tuning Configurations.** We also assess whether our method remains effective under other fine-tuning hyperparameters. Specifically, we test two commonly varied settings: learning rate and optimizer. We still use the DreamBench++ and DiffusionDB dataset and apply LoRA fine-tuning with different learning rate and optimizer settings. As shown in Tab. 4 and 5, ResAlign continues to perform well across these configurations, maintaining low harmfulness across different settings. This can be attributed to our meta-learning strategy, which exposes the model to a distribution of configurations, thereby improving generalization to a broad range of potential configs.

**Effectiveness on Contaminated Data.** Lastly, we consider a challenging scenario where the fine-tuning data is either intentionally or inadvertently contaminated with unsafe content. To evaluate this, we mix our datasets with the Harmful-Imgs dataset [51] at varying contamination ratios, and use this contaminated data to fine-tune the unlearned models. As shown in Fig. 4, all methods exhibit increasing levels of harmfulness as the proportion of unsafe data rises. Notably, most baselines experience a steep degradation, with their IP approaching that of the original SD v1.4 when 20% or more of the data is unsafe. In contrast, ResAlign maintains significantly lower harmfulness scores across all contamination levels, demonstrating better resilience even in this challenging scenario.



Tab. 4: Effectiveness of ResAlign under various fine-tuning learning rates. Adapt. refers to an adaptive learning rate scheduler that initiates at  $5 \times 10^{-3}$  and gradually decays using cosine annealing down to the minimum learning rate of  $1 \times 10^{-6}$ . The reported metric is IP after fine-tuning.

Dataset	$1 \times 10^{-3}$	$5 \times 10^{-4}$	$1 \times 10^{-4}$	$5 \times 10^{-5}$	$1 \times 10^{-5}$	$5 \times 10^{-6}$	Adapt.
DreamBench++	0.018	0.002	0.004	0.004	0.001	0.002	0.011
DiffusionDB	0.059	0.053	0.043	0.054	0.069	0.044	0.059

Tab. 5: Effectiveness of ResAlign under various fine-tuning optimizers. The metric is IP after fine-tuning.

Optimizer	DB++	Diff.DB
SGD	0.0004	0.0118
Adam	0.0014	0.0687
AdamW	0.0026	0.0478

Overall, we argue perfect resilience against harmful data is inherently difficult—if not impossible—as, an adversary can, after all, treat the recovery of unsafe behavior as a new learning task [9], which pre-trained diffusion models are adept at due to their strong generalization and few-shot learning capability [64, 34]. Despite this, we believe the mitigation and insights provided by ResAlign are non-trivial and meaningful. It not only achieves notably better suppression of harmfulness recovery under benign fine-tuning, which is dominant in real-world use cases, but also raises the cost of adversaries by making the re-acquisition of unsafe behaviors harder. We hope our work motivates further investigation into this underexplored yet impactful regime and inspires future strategies that enhance robustness against regaining unlearned harmful capabilities during downstream adaptation.

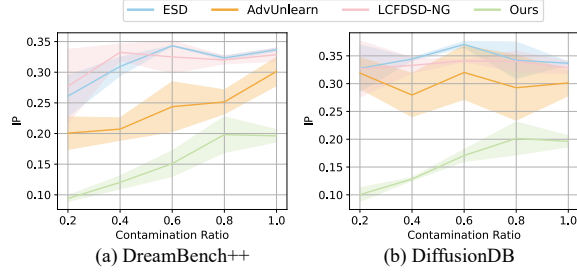


Fig. 4: Evaluation on contaminated data.

**Ablation Study.** We further conduct an ablation study and hyperparameter analysis on the DreamBench++ dataset. From Tab. 3, we can see that every component contributes to our ResAlign, with hypergradient approximation (Hyper.) enabling reducing regained harmfulness and meta-learning on dataset (Meta. (D)) and configurations (Meta. (C)) notably mitigate overfitting and enhance generalization. Besides, the hyperparameter  $\gamma$  controls the degree of proximity to the base model. A larger  $\gamma$  can better approximate the ground-truth fine-tuned model, yet also leads to higher instability due to larger variance in hypergradient approximation, as shown in Fig. 5. Overall, our method is stable when  $\gamma$  is in a reasonable range (i.e.,  $0 \sim 1$ ). Thus, a wide range of  $\gamma$  can be selected for ResAlign.

Tab. 3: Effect of components.

Component			Metric	
Hyper.	Meta. (D)	Meta. (C)	IP ↓	FID ↓
—	—	—	0.2266	18.24
✓	—	—	0.1826	18.07
✓	✓	—	0.0322	18.35
✓	✓	✓	0.0186	18.18

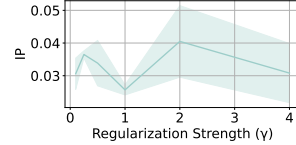


Fig. 5: Effect of  $\gamma$ .

## 5 Conclusion

This paper proposes ResAlign, a novel unlearning framework designed to enhance the resilience of unlearned diffusion models against downstream fine-tuning. Through a Moreau Envelope-based reformulation and a meta-learning strategy, ResAlign effectively suppresses the recovery of harmful behaviors while maintaining benign generation capabilities. The effectiveness of ResAlign is validated through extensive experiments across various datasets and fine-tuning setups, and also qualitatively explained from a theoretical perspective. We hope our work can raise community attention to the resilience of unlearning methods and encourage further research into more robust strategies.

**Ethics Statement.** This work explores the safety risks of safety-driven unlearned text-to-image diffusion models, particularly their susceptibility of regaining unsafe behaviors after downstream fine-tuning. Our main contribution is ResAlign, a novel framework that enhances the resilience of safety-driven unlearning, mitigating the reemergence of harmful outputs after downstream fine-tuning, which is a defense mechanism. We are confident that our research complies with ethical standards. All experiments are conducted on publicly available datasets, and potentially harmful visualizations are intentionally blurred or blocked. Our method is developed solely to promote the safe and responsible use of generative models and is not intended for any malicious or unethical applications.

## References

- [1] Safinah Ali, Daniella DiPaola, Randi Williams, Prerna Ravi, and Cynthia Breazeal. Constructing dreams using generative ai. *arXiv preprint arXiv:2305.12013*, 2023.
- [2] Ron Amit and Ron Meir. Meta-learning by adjusting priors based on extended pac-bayes theory. In *International Conference on Machine Learning*, pages 205–214. PMLR, 2018.
- [3] Maksym Andriushchenko and Nicolas Flammarion. Understanding and improving fast adversarial training. *Advances in Neural Information Processing Systems*, 33:16048–16059, 2020.
- [4] Yu Bai, Ben Krause, Huan Wang, Caiming Xiong, and Richard Socher. Taylorized training: Towards better approximation of neural network training at finite width. *arXiv preprint arXiv:2002.04010*, 2020.
- [5] Xinlei Chen, Hao Fang, Tsung-Yi Lin, Ramakrishna Vedantam, Saurabh Gupta, Piotr Dollár, and C Lawrence Zitnick. Microsoft coco captions: Data collection and evaluation server. *arXiv preprint arXiv:1504.00325*, 2015.
- [6] Xuanhong Chen, Bingbing Ni, Yutian Liu, Naiyuan Liu, Zhilin Zeng, and Hang Wang. Sim-swap++: Towards faster and high-quality identity swapping. *IEEE Transactions on Pattern Analysis and Machine Intelligence*, 46(1):576–592, 2023.
- [7] Civitai. Civitai: A platform for sharing and discovering ai-generated art models, 2025. Accessed: 2025-05-15.
- [8] CompVis. Stable diffusion safety checker. <https://huggingface.co/CompVis/stable-diffusion-safety-checker>, 2022. Accessed: 2025-03-21.
- [9] Jiangyi Deng, Shengyuan Pang, Yanjiao Chen, Liangming Xia, Yijie Bai, Haiqin Weng, and Wenyan Xu. Sophon: Non-fine-tunable learning to restrain task transferability for pre-trained models. In *2024 IEEE Symposium on Security and Privacy (SP)*, pages 2553–2571. IEEE, 2024.
- [10] Laurent Dinh, Razvan Pascanu, Samy Bengio, and Yoshua Bengio. Sharp minima can generalize for deep nets. In *International Conference on Machine Learning*, pages 1019–1028. PMLR, 2017.
- [11] Pierre Fernandez, Guillaume Couairon, Hervé Jégou, Matthijs Douze, and Teddy Furon. The stable signature: Rooting watermarks in latent diffusion models. In *Proceedings of the IEEE/CVF International Conference on Computer Vision*, pages 22466–22477, 2023.
- [12] Chelsea Finn, Pieter Abbeel, and Sergey Levine. Model-agnostic meta-learning for fast adaptation of deep networks. In *International conference on machine learning*, pages 1126–1135. PMLR, 2017.
- [13] Pierre Foret, Ariel Kleiner, Hossein Mobahi, and Behnam Neyshabur. Sharpness-aware minimization for efficiently improving generalization. *arXiv preprint arXiv:2010.01412*, 2020.
- [14] Pierre Foret, Ariel Kleiner, Hossein Mobahi, and Behnam Neyshabur. Sharpness-aware minimization for efficiently improving generalization. In *International Conference on Learning Representations*, 2021.
- [15] Stanislav Fort, Huiyi Hu, and Balaji Lakshminarayanan. Deep ensembles: A loss landscape perspective. *arXiv preprint arXiv:1912.02757*, 2019.
- [16] Zihao Fu, Anthony Man-Cho So, and Nigel Collier. A stability analysis of fine-tuning a pre-trained model. *arXiv preprint arXiv:2301.09820*, 2023.
- [17] Zihao Fu, Haoran Yang, Anthony Man-Cho So, Wai Lam, Lidong Bing, and Nigel Collier. On the effectiveness of parameter-efficient fine-tuning. In *Proceedings of the AAAI conference on artificial intelligence*, volume 37, pages 12799–12807, 2023.

- [18] Rohit Gandikota, Joanna Materzynska, Jaden Fiotto-Kaufman, and David Bau. Erasing concepts from diffusion models. In *Proceedings of the IEEE/CVF International Conference on Computer Vision*, pages 2426–2436, 2023.
- [19] Rohit Gandikota, Hadas Orgad, Yonatan Belinkov, Joanna Materzyńska, and David Bau. Unified concept editing in diffusion models. In *Proceedings of the IEEE/CVF Winter Conference on Applications of Computer Vision*, pages 5111–5120, 2024.
- [20] Hongcheng Gao, Tianyu Pang, Chao Du, Taihang Hu, Zhijie Deng, and Min Lin. Meta-unlearning on diffusion models: Preventing relearning unlearned concepts. *arXiv preprint arXiv:2410.12777*, 2024.
- [21] Lucy L Gao, Jane J Ye, Haian Yin, Shangzhi Zeng, and Jin Zhang. Moreau envelope based difference-of-weakly-convex reformulation and algorithm for bilevel programs. *arXiv preprint arXiv:2306.16761*, 2023.
- [22] Chao Gong, Kai Chen, Zhipeng Wei, Jingjing Chen, and Yu-Gang Jiang. Reliable and efficient concept erasure of text-to-image diffusion models. In *European Conference on Computer Vision*, pages 73–88. Springer, 2024.
- [23] Ligong Han, Yinxiao Li, Han Zhang, Peyman Milanfar, Dimitris Metaxas, and Feng Yang. Svdiff: Compact parameter space for diffusion fine-tuning. In *Proceedings of the IEEE/CVF International Conference on Computer Vision*, pages 7323–7334, 2023.
- [24] Martin Heusel, Hubert Ramsauer, Thomas Unterthiner, Bernhard Nessler, and Sepp Hochreiter. Gans trained by a two time-scale update rule converge to a local nash equilibrium. *NeurIPS*, 2017.
- [25] Jonathan Ho, Ajay Jain, and Pieter Abbeel. Denoising diffusion probabilistic models. *Advances in neural information processing systems*, 33:6840–6851, 2020.
- [26] Edward J Hu, Yelong Shen, Phillip Wallis, Zeyuan Allen-Zhu, Yanzhi Li, Shean Wang, Lu Wang, Weizhu Chen, et al. Lora: Low-rank adaptation of large language models. *ICLR*, 1(2):3, 2022.
- [27] Michael F Hutchinson. A stochastic estimator of the trace of the influence matrix for laplacian smoothing splines. *Communications in Statistics-Simulation and Computation*, 18(3):1059–1076, 1989.
- [28] Pavel Izmailov, Dmitrii Podoprikin, Timur Garipov, Dmitry Vetrov, and Andrew Gordon Wilson. Averaging weights leads to wider optima and better generalization. *arXiv preprint arXiv:1803.05407*, 2018.
- [29] Arthur Jacot, Franck Gabriel, and Clément Hongler. Neural tangent kernel: Convergence and generalization in neural networks. *Advances in neural information processing systems*, 31, 2018.
- [30] Nitish Shirish Keskar, Dheevatsa Mudigere, Jorge Nocedal, Mikhail Smelyanskiy, and Ping Tak Peter Tang. On large-batch training for deep learning: Generalization gap and sharp minima. *arXiv preprint arXiv:1609.04836*, 2016.
- [31] James Kirkpatrick, Razvan Pascanu, Neil Rabinowitz, Joel Veness, Guillaume Desjardins, Andrei A Rusu, Kieran Milan, John Quan, Tiago Ramalho, Agnieszka Grabska-Barwinska, et al. Overcoming catastrophic forgetting in neural networks. *Proceedings of the national academy of sciences*, 114(13):3521–3526, 2017.
- [32] Harold W Kuhn and Albert W Tucker. Nonlinear programming. In *Traces and emergence of nonlinear programming*, pages 247–258. Springer, 2013.
- [33] Nupur Kumari, Bingliang Zhang, Sheng-Yu Wang, Eli Shechtman, Richard Zhang, and Jun-Yan Zhu. Ablating concepts in text-to-image diffusion models. In *Proceedings of the IEEE/CVF International Conference on Computer Vision*, pages 22691–22702, 2023.

- [34] Nupur Kumari, Bingliang Zhang, Richard Zhang, Eli Shechtman, and Jun-Yan Zhu. Multi-concept customization of text-to-image diffusion. In *Proceedings of the IEEE/CVF conference on computer vision and pattern recognition*, pages 1931–1941, 2023.
- [35] LAION-AI. Laion-aesthetics-predictor v1. <https://github.com/LAION-AI/aesthetic-predictor>, 2022. Accessed: 2025-05-14.
- [36] Jaehoon Lee, Lechao Xiao, Samuel Schoenholz, Yasaman Bahri, Roman Novak, Jascha Sohl-Dickstein, and Jeffrey Pennington. Wide neural networks of any depth evolve as linear models under gradient descent. *Advances in neural information processing systems*, 32, 2019.
- [37] Boheng Li, Yanhao Wei, Yankai Fu, Zhenting Wang, Yiming Li, Jie Zhang, Run Wang, and Tianwei Zhang. Towards reliable verification of unauthorized data usage in personalized text-to-image diffusion models. In *2025 IEEE Symposium on Security and Privacy (SP)*, pages 73–73. IEEE Computer Society, 2024.
- [38] Guanlin Li, Kangjie Chen, Shudong Zhang, Jie Zhang, and Tianwei Zhang. Art: Automatic red-teaming for text-to-image models to protect benign users. In *The Thirty-eighth Annual Conference on Neural Information Processing Systems*, 2024.
- [39] Xinfeng Li, Yuchen Yang, Jiangyi Deng, Chen Yan, Yanjiao Chen, Xiaoyu Ji, and Wenyan Xu. Safegen: Mitigating sexually explicit content generation in text-to-image models. In *Proceedings of the 2024 on ACM SIGSAC Conference on Computer and Communications Security*, pages 4807–4821, 2024.
- [40] Yiming Li, Shuo Shao, Yu He, Junfeng Guo, Tianwei Zhang, Zhan Qin, Pin-Yu Chen, Michael Backes, Philip Torr, Dacheng Tao, and Kui Ren. Rethinking data protection in the (generative) artificial intelligence era. *arXiv preprint arXiv:2507.03034*, 2025.
- [41] Peiyuan Liao, Xiuyu Li, Xihui Liu, and Kurt Keutzer. The artbench dataset: Benchmarking generative models with artworks. *arXiv preprint arXiv:2206.11404*, 2022.
- [42] Risheng Liu, Zhu Liu, Wei Yao, Shangzhi Zeng, and Jin Zhang. Moreau envelope for non-convex bi-level optimization: A single-loop and hessian-free solution strategy. In *Forty-first International Conference on Machine Learning*, 2024.
- [43] Runtao Liu, Ashkan Khakzar, Jindong Gu, Qifeng Chen, Philip Torr, and Fabio Pizzati. Latent guard: a safety framework for text-to-image generation. In *European Conference on Computer Vision*, pages 93–109. Springer, 2024.
- [44] Yixin Liu, Chenrui Fan, Yutong Dai, Xun Chen, Pan Zhou, and Lichao Sun. Metacloak: Preventing unauthorized subject-driven text-to-image diffusion-based synthesis via meta-learning. In *Proceedings of the IEEE/CVF Conference on Computer Vision and Pattern Recognition*, pages 24219–24228, 2024.
- [45] Sadhika Malladi, Alexander Wettig, Dingli Yu, Danqi Chen, and Sanjeev Arora. A kernel-based view of language model fine-tuning. In *International Conference on Machine Learning*, pages 23610–23641. PMLR, 2023.
- [46] Common Sense Media. Most us teens use generative ai. most of their parents don’t know. *Wired*, 2024.
- [47] Jean-Jacques Moreau. Proximité et dualité dans un espace hilbertien. *Bulletin de la Société mathématique de France*, 93:273–299, 1965.
- [48] Alex Nichol, Joshua Achiam, and John Schulman. On first-order meta-learning algorithms. *arXiv preprint arXiv:1803.02999*, 2018.
- [49] Maxime Oquab, Timothée Darcet, Théo Moutakanni, Huy V. Vo, Marc Szafraniec, Vasil Khalidov, Pierre Fernandez, Daniel HAZIZA, Francisco Massa, Alaaeldin El-Nouby, Mido Assran, Nicolas Ballas, Wojciech Galuba, Russell Howes, Po-Yao Huang, Shang-Wen Li, Ishan Misra, Michael Rabbat, Vasu Sharma, Gabriel Synnaeve, Hu Xu, Herve Jegou, Julien Mairal, Patrick Labatut, Armand Joulin, and Piotr Bojanowski. DINOv2: Learning robust visual features without supervision. *TMLR*, 2024.



- [50] Guillermo Ortiz-Jimenez, Alessandro Favero, and Pascal Frossard. Task arithmetic in the tangent space: Improved editing of pre-trained models. *Advances in Neural Information Processing Systems*, 36:66727–66754, 2023.
- [51] Jiadong Pan, Hongcheng Gao, Zongyu Wu, Taihang Hu, Li Su, Qingming Huang, and Liang Li. Leveraging catastrophic forgetting to develop safe diffusion models against malicious finetuning. *Advances in Neural Information Processing Systems*, 37:115208–115232, 2024.
- [52] Yuang Peng, Yuxin Cui, Haomiao Tang, Zekun Qi, Runpei Dong, Jing Bai, Chunrui Han, Zheng Ge, Xiangyu Zhang, and Shu-Tao Xia. Dreambench++: A human-aligned benchmark for personalized image generation. In *The Thirteenth International Conference on Learning Representations*, 2025.
- [53] platelminto. Nudenetclassifier. <https://github.com/platelminto/NudeNetClassifier>, 2021. Accessed: 2025-03-21.
- [54] Dustin Podell, Zion English, Kyle Lacey, Andreas Blattmann, Tim Dockhorn, Jonas Müller, Joe Penna, and Robin Rombach. Sdxl: Improving latent diffusion models for high-resolution image synthesis. In *The Twelfth International Conference on Learning Representations*, 2024.
- [55] Wenjie Qu, Wengrui Zheng, Tianyang Tao, Dong Yin, Yanze Jiang, Zhihua Tian, Wei Zou, Jinyuan Jia, and Jiaheng Zhang. Provably robust multi-bit watermarking for ai-generated text. *arXiv preprint arXiv:2401.16820*, 2024.
- [56] Yiting Qu, Xinyue Shen, Xinlei He, Michael Backes, Savvas Zannettou, and Yang Zhang. Unsafe diffusion: On the generation of unsafe images and hateful memes from text-to-image models. In *Proceedings of the 2023 ACM SIGSAC conference on computer and communications security*, pages 3403–3417, 2023.
- [57] Alec Radford, Jong Wook Kim, Chris Hallacy, Aditya Ramesh, Gabriel Goh, Sandhini Agarwal, Girish Sastry, Amanda Askell, Pamela Mishkin, Jack Clark, et al. Learning transferable visual models from natural language supervision. In *ICML*, 2021.
- [58] Evani Radiya-Dixit and Xin Wang. How fine can fine-tuning be? learning efficient language models. In *International Conference on Artificial Intelligence and Statistics*, pages 2435–2443. PMLR, 2020.
- [59] Aravind Rajeswaran, Chelsea Finn, Sham M Kakade, and Sergey Levine. Meta-learning with implicit gradients. *Advances in neural information processing systems*, 32, 2019.
- [60] Javier Rando, Daniel Paleka, David Lindner, Lennart Heim, and Florian Tramer. Red-teaming the stable diffusion safety filter. In *NeurIPS ML Safety Workshop*, 2022.
- [61] reach vb. Pokémon blip captions. <https://huggingface.co/datasets/reach-vb/pokemon-blip-captions>, 2023. Accessed: 2025-05-14.
- [62] Lewis Fry Richardson. IX. the approximate arithmetical solution by finite differences of physical problems involving differential equations, with an application to the stresses in a masonry dam. *Philosophical Transactions of the Royal Society of London. Series A, containing papers of a mathematical or physical character*, 210(459-470):307–357, 1911.
- [63] Robin Rombach, Andreas Blattmann, Dominik Lorenz, Patrick Esser, and Björn Ommer. High-resolution image synthesis with latent diffusion models. In *Proceedings of the IEEE/CVF conference on computer vision and pattern recognition*, pages 10684–10695, 2022.
- [64] Nataniel Ruiz, Yuanzhen Li, Varun Jampani, Yael Pritch, Michael Rubinstein, and Kfir Aberman. Dreambooth: Fine tuning text-to-image diffusion models for subject-driven generation. In *Proceedings of the IEEE/CVF conference on computer vision and pattern recognition*, pages 22500–22510, 2023.
- [65] Patrick Schramowski, Manuel Brack, Björn Deiseroth, and Kristian Kersting. Safe latent diffusion: Mitigating inappropriate degeneration in diffusion models. In *Proceedings of the IEEE/CVF Conference on Computer Vision and Pattern Recognition*, pages 22522–22531, 2023.

- [66] Patrick Schramowski, Christopher Tauchmann, and Kristian Kersting. Can machines help us answering question 16 in datasheets, and in turn reflecting on inappropriate content? In *Proceedings of the 2022 ACM conference on fairness, accountability, and transparency*, pages 1350–1361, 2022.
- [67] Christoph Schuhmann, Romain Beaumont, Richard Vencu, Cade Gordon, Ross Wightman, Mehdi Cherti, Theo Coombes, Aarush Katta, Clayton Mullis, Mitchell Wortsman, et al. Laion-5b: An open large-scale dataset for training next generation image-text models. *Advances in neural information processing systems*, 35:25278–25294, 2022.
- [68] Mandt Stephan, Matthew D Hoffman, David M Blei, et al. Stochastic gradient descent as approximate bayesian inference. *Journal of Machine Learning Research*, 18(134):1–35, 2017.
- [69] Anke Tang, Li Shen, Yong Luo, Yibing Zhan, Han Hu, Bo Du, Yixin Chen, and Dacheng Tao. Parameter efficient multi-task model fusion with partial linearization. *arXiv preprint arXiv:2310.04742*, 2023.
- [70] Yiyang Wang and Weining Zhang. Factors influencing the adoption of generative ai for art designing among chinese generation z: A structural equation modeling approach. *IEEE Access*, 11:143272–143284, 2023.
- [71] Zijie J Wang, Evan Montoya, David Munechika, Haoyang Yang, Benjamin Hoover, and Duen Horng Chau. Diffusiondb: A large-scale prompt gallery dataset for text-to-image generative models. In *Proceedings of the 61st Annual Meeting of the Association for Computational Linguistics (Volume 1: Long Papers)*, pages 893–911, 2023.
- [72] Zilan Wang, Junfeng Guo, Jiacheng Zhu, Yiming Li, Heng Huang, Muhao Chen, and Zhengzhong Tu. Sleepermark: Towards robust watermark against fine-tuning text-to-image diffusion models. In *Proceedings of the Computer Vision and Pattern Recognition Conference*, pages 8213–8224, 2025.
- [73] Jiancong Xiao, Jiawei Zhang, Zhi-Quan Luo, and Asuman E. Ozdaglar. Uniformly stable algorithms for adversarial training and beyond. In *Forty-first International Conference on Machine Learning*, 2024.
- [74] Yijun Yang, Ruiyuan Gao, Xiao Yang, Jianyuan Zhong, and Qiang Xu. Guardt2i: Defending text-to-image models from adversarial prompts. In *The Thirty-eighth Annual Conference on Neural Information Processing Systems*, 2024.
- [75] Yuchen Yang, Bo Hui, Haolin Yuan, Neil Gong, and Yinzhi Cao. Sneakyprompt: Jailbreaking text-to-image generative models. In *2024 IEEE symposium on security and privacy (SP)*, pages 897–912. IEEE, 2024.
- [76] Jaesik Yoon, Taesup Kim, Ousmane Dia, Sungwoong Kim, Yoshua Bengio, and Sungjin Ahn. Bayesian model-agnostic meta-learning. *Advances in neural information processing systems*, 31, 2018.
- [77] Kaibo Zhang, Yunjuan Wang, and Raman Arora. Stability and generalization of adversarial training for shallow neural networks with smooth activation. *Advances in Neural Information Processing Systems*, 37:16160–16193, 2024.
- [78] Yimeng Zhang, Xin Chen, Jinghan Jia, Yihua Zhang, Chongyu Fan, Jiancheng Liu, Mingyi Hong, Ke Ding, and Sijia Liu. Defensive unlearning with adversarial training for robust concept erasure in diffusion models. *Advances in Neural Information Processing Systems*, 37:36748–36776, 2024.
- [79] Yimeng Zhang, Jinghan Jia, Xin Chen, Aochuan Chen, Yihua Zhang, Jiancheng Liu, Ke Ding, and Sijia Liu. To generate or not? safety-driven unlearned diffusion models are still easy to generate unsafe images... for now. In *European Conference on Computer Vision*, pages 385–403. Springer, 2024.
- [80] Amber Yijia Zheng and Raymond A Yeh. Imma: Immunizing text-to-image models against malicious adaptation. In *European Conference on Computer Vision*, pages 458–475. Springer, 2024.

## A Omitted Proofs & Derivations

### A.1 Omitted Derivation for Eq. (6)

Recall that we approximate the parameters obtained via finite-step fine-tuning from a pretrained model using the following Moreau Envelope (ME) formulation:

$$\theta_{\text{FT}}^* \in \arg \min_{\theta'} \mathcal{L}_{\text{FT}}(\theta', \mathcal{D}_{\text{FT}}) + \frac{1}{2\gamma} \|\theta' - \theta\|^2 \quad (9)$$

As  $\theta_{\text{FT}}^*$  is the minimizer of the above optimization problem, it satisfies the following first-order optimality condition according to the KKT theorem:

$$\nabla_{\theta'} \mathcal{L}_{\text{FT}}(\theta_{\text{FT}}^*, \mathcal{D}_{\text{FT}}) + \frac{1}{\gamma} (\theta_{\text{FT}}^* - \theta) = 0 \quad (10)$$

Define a function  $F(\theta', \theta) = \nabla_{\theta'} \mathcal{L}_{\text{FT}}(\theta', \mathcal{D}_{\text{FT}}) + \frac{1}{\gamma} (\theta' - \theta)$ . The optimality condition implies that  $F(\theta_{\text{FT}}^*, \theta) = 0$ . Since  $\theta_{\text{FT}}^*$  is implicitly defined as a function of  $\theta$  through this equation, we can apply the Implicit Function Theorem (IFT) to compute how  $\theta_{\text{FT}}^*$  changes with respect to  $\theta$ . Specifically, IFT states that if  $F(\theta', \theta) = 0$  and  $\nabla_{\theta'} F$  is invertible at  $\theta_{\text{FT}}^*$ , then:

$$\frac{\partial \theta_{\text{FT}}^*}{\partial \theta} = - \left( \frac{\partial F}{\partial \theta'} \right)^{-1} \cdot \frac{\partial F}{\partial \theta} \quad (11)$$

We compute the two Jacobians of  $F$  as follows:

$$\frac{\partial F}{\partial \theta'} = \nabla_{\theta'}^2 \mathcal{L}_{\text{FT}}(\theta_{\text{FT}}^*, \mathcal{D}_{\text{FT}}) + \frac{1}{\gamma} I, \quad \frac{\partial F}{\partial \theta} = -\frac{1}{\gamma} I \quad (12)$$

Substituting into Eq. (11), we obtain:

$$\frac{\partial \theta_{\text{FT}}^*}{\partial \theta} = \left( \nabla_{\theta'}^2 \mathcal{L}_{\text{FT}}(\theta_{\text{FT}}^*, \mathcal{D}_{\text{FT}}) + \frac{1}{\gamma} I \right)^{-1} \cdot \frac{1}{\gamma} I \quad (13)$$

Now consider the loss function  $\mathcal{L}_{\text{harmful}}(\theta_{\text{FT}}^*)$ . By the chain rule:

$$\nabla_{\theta} \mathcal{L}_{\text{harmful}}(\theta_{\text{FT}}^*) = \left( \frac{\partial \theta_{\text{FT}}^*}{\partial \theta} \right)^{\top} \cdot \nabla_{\theta_{\text{FT}}^*} \mathcal{L}_{\text{harmful}}(\theta_{\text{FT}}^*) \quad (14)$$

Then, since the Jacobian matrix is symmetric (as it involves the inverse of a symmetric positive definite matrix), we simplify:

$$\nabla_{\theta} \mathcal{L}_{\text{harmful}}(\theta_{\text{FT}}^*) = \left( \nabla_{\theta'}^2 \mathcal{L}_{\text{FT}}(\theta_{\text{FT}}^*, \mathcal{D}_{\text{FT}}) + \frac{1}{\gamma} I \right)^{-1} \cdot \frac{1}{\gamma} \cdot \nabla_{\theta_{\text{FT}}^*} \mathcal{L}_{\text{harmful}}(\theta_{\text{FT}}^*) \quad (15)$$

Finally, multiplying both sides by the inverse term's denominator yields:

$$\left( \nabla_{\theta_{\text{FT}}^*}^2 \mathcal{L}_{\text{FT}}(\theta_{\text{FT}}^*, \mathcal{D}_{\text{FT}}) + \frac{1}{\gamma} I \right) \cdot \nabla_{\theta} \mathcal{L}_{\text{harmful}}(\theta_{\text{FT}}^*) = \frac{1}{\gamma} \nabla_{\theta_{\text{FT}}^*} \mathcal{L}_{\text{harmful}}(\theta_{\text{FT}}^*) \quad (16)$$

Noting that  $\theta'$  is evaluated at its optimal value  $\theta_{\text{FT}}^*$ , we equivalently write  $\nabla_{\theta'}^2 \mathcal{L}_{\text{FT}}(\theta_{\text{FT}}^*, \mathcal{D}_{\text{FT}})$  as  $\nabla_{\theta_{\text{FT}}^*}^2 \mathcal{L}_{\text{FT}}(\theta_{\text{FT}}^*, \mathcal{D}_{\text{FT}})$  for clarity. This concludes the derivation.  $\square$

A derivation similar to ours was presented by Rajeswaran et al. [59] in the context of meta-learning. Specifically, they model the lower-level transfer (or adaptation) step in meta-learning as a proximal regularized optimization process, which is conceptually similar to our Moreau Envelope-based formulation. This allows them to compute the meta-gradients with respect to the meta-parameters through implicit differentiation, a technique that shares structural similarity with our derivation above. However, while the underlying mathematical tools overlap, our goals and problem settings are fundamentally distinct. The primary objective in Rajeswaran et al. [59] is to strengthen task-level adaptability in meta-learned models. In contrast, our method is developed to enhance resilience against the reemergence of unsafe behaviors during downstream fine-tuning of generative models.

## A.2 Omitted Proof for Proposition 1

*Proof.* Prior works have shown that fine-tuning typically induces only small parameter changes to the pretrained parameters [58, 16, 4, 69, 17]. As a result, the fine-tuned parameters can be represented as a sufficiently small additive perturbation of the pretrained ones [45, 17, 58], i.e.,  $\theta_{\text{FT}}^* = \theta + \xi$ , where  $\xi = \sigma z^2$ . By the second-order Taylor expansion around  $\theta$  and dropping higher-order terms:

$$\begin{aligned}\mathcal{L}_{\text{harmful}}(\theta_{\text{FT}}^*) &= \mathcal{L}_{\text{harmful}}(\theta + \xi) \\ &\approx \mathcal{L}_{\text{harmful}}(\theta) + \nabla_{\theta} \mathcal{L}_{\text{harmful}}(\theta)^{\top} \xi + \frac{1}{2} \xi^{\top} \nabla_{\theta}^2 \mathcal{L}_{\text{harmful}}(\theta) \xi.\end{aligned}\quad (17)$$

Because  $z$  is a unit random variable, we have  $\mathbb{E}[z] = 0$ . Then, taking expectation over  $z$ , we obtain:

$$\begin{aligned}\mathbb{E}[\mathcal{L}_{\text{harmful}}(\theta_{\text{FT}}^*) - \mathcal{L}_{\text{harmful}}(\theta)] &\approx \sigma \nabla_{\theta} \mathcal{L}_{\text{harmful}}(\theta)^{\top} \mathbb{E}[z] + \frac{\sigma^2}{2} \mathbb{E}[z^{\top} \nabla_{\theta}^2 \mathcal{L}_{\text{harmful}}(\theta) z] \\ &= \frac{\sigma^2}{2} \cdot \mathbb{E}[z^{\top} \nabla_{\theta}^2 \mathcal{L}_{\text{harmful}}(\theta) z].\end{aligned}\quad (18)$$

To compute this expectation, we use the fact that for any symmetric matrix  $H$  and random vector  $z$  with  $\mathbb{E}[zz^{\top}] = \frac{1}{d}I$ , we have:

$$\mathbb{E}[z^{\top} H z] = \text{Tr}(\mathbb{E}[zz^{\top}] H) = \text{Tr}\left(\frac{1}{d}I \cdot H\right) = \frac{1}{d} \text{Tr}(H).\quad (19)$$

Applying this to  $H = \nabla_{\theta}^2 \mathcal{L}_{\text{harmful}}(\theta)$ , we obtain:

$$\mathbb{E}[z^{\top} \nabla_{\theta}^2 \mathcal{L}_{\text{harmful}}(\theta) z] = \frac{1}{d} \text{Tr}(\nabla_{\theta}^2 \mathcal{L}_{\text{harmful}}(\theta)).\quad (20)$$

Hence, substituting into Eq. (18), we obtain the following expression:

$$\mathbb{E}[\mathcal{L}_{\text{harmful}}(\theta_{\text{FT}}^*) - \mathcal{L}_{\text{harmful}}(\theta)] \approx \frac{\sigma^2}{2d} \cdot \text{Tr}(\nabla_{\theta}^2 \mathcal{L}_{\text{harmful}}(\theta)).\quad (21)$$

Since the term  $\frac{\sigma^2}{2d}$  is a constant independent of  $\theta$ , minimizing the expected regained harmful loss is equivalent to minimizing the trace of the Hessian matrix:

$$\arg \min_{\theta} \mathbb{E}[\mathcal{L}_{\text{harmful}}(\theta_{\text{FT}}^*) - \mathcal{L}_{\text{harmful}}(\theta)] \approx \arg \min_{\theta} \text{Tr}(\nabla_{\theta}^2 \mathcal{L}_{\text{harmful}}(\theta)).\quad (22)$$

Thus, we finished the proof.  $\square$

**Remarks & Discussions.** Proposition 1 suggests that our proposed additive term implicitly penalizes the trace of the Hessian of the harmful loss near the unlearned model parameters. In doing so, it encourages the optimization process not only to minimize the harmful loss, but also to favor solutions with flatter local geometry, i.e., regions with lower curvature. This intuition is illustrated in Fig. 6. While prior unlearning methods aim to reduce  $\mathcal{L}_{\text{harmful}}$ , they typically rely on standard SGD-based optimizers, which are known to prefer sharp local minima [30]. As a result, these methods may converge to parameter regions such as  $\theta_{\text{unlearn}}^{*}$  that, although locally optimal, are highly sensitive to downstream perturbations. As a result, even benign fine-tuning, which aims to optimize only the benign loss  $\mathcal{L}_{\text{FT}}$  (i.e., aim to pushing  $\theta_{\text{unlearn}}^{*}$  to  $\theta_{\text{FT}}^*$ ), may inadvertently push the model back into regions of high harmful loss, reactivating undesired behaviors.

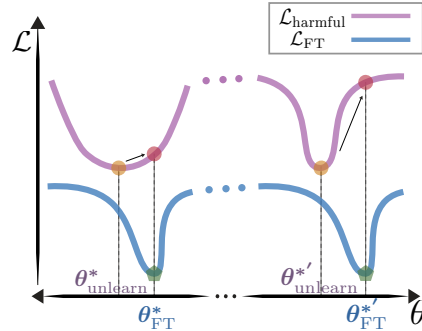


Fig. 6: Illustration of the impact of (benign) fine-tuning on harmful loss for flat (left) and sharp (right) minima.

<sup>2</sup>Here, unlike many previous works that restrictively assume  $z$  to follow a specific distribution (e.g., Gaussian [15, 28] or uniform on the sphere [10, 3]), or confining analysis to first-order approximations like the Neural Tangent Kernel (NTK) [36, 50, 29], we only assume the additive perturbation is a scaled unit random variable, i.e., any distribution satisfying  $\mathbb{E}[z] = 0$  and  $\mathbb{E}[zz^{\top}] = \frac{1}{d}I$ , which is a milder and more flexible assumption.



In contrast, our ResAlign method implicitly promotes flatter optima (e.g.,  $\theta_{\text{unlearn}}^*$  in the figure). These flatter solutions are more resilient to subsequent fine-tuning: local updates to minimize  $\mathcal{L}_{\text{FT}}$  induce smaller changes in  $\mathcal{L}_{\text{harmful}}$ , thereby reducing the risk of unlearning failure. This perspective suggests that the fragility of prior unlearning methods may arise not from the nature of the downstream data itself, but from the sharpness of the solutions they converge to.

With that being said, we acknowledge that our proposition, like other analyses based on Taylor expansions and additive perturbation models [29, 31, 13], may become less accurate in scenarios involving large parameter shifts (e.g., very large learning rates or very long fine-tuning schedules), or when the perturbation lacks a well-behaved distribution [31, 68]. Nonetheless, in practice, particularly in diffusion model fine-tuning setting, small learning rates and moderate step sizes are commonly used to preserve generative quality and prevent overfitting [64, 23, 26], which supports the validity of the small perturbation assumption. Moreover, since our meta-learning process is performed over diverse data sampling and configurations, modeling  $\xi$  as an isotropic random variable is a reasonable abstraction, as widely adopted by previous works [76, 2, 59]. As one of the earliest attempts to theoretically understand the interplay between unlearning and subsequent fine-tuning, our analysis is meant to provide a qualitative, approximate explanation rather than definitive conclusions. We hope our work can inspire the community to pursue deeper and more precise theoretical investigations into the robustness of unlearning under realistic deployment conditions.

## B Discussion

### B.1 Limitations & Future Work

Our work still has the following limitations, which we aim to address in future work. First, our approach requires simulating fine-tuning during the unlearning process, which introduces additional computational overhead. However, the total cost remains within a practical range ( $\sim 56$  GPU minutes for a full run in our main experiments), which is significantly more efficient than retraining a model from scratch. In real-world scenarios, users can choose methods that best balance their needs for resilience and safety given their computational budget. Second, our Moreau envelope-based approximation is inherently an approximation. Nevertheless, our experiments show that it is robust to long fine-tuning steps and a wide range of learning rates, and it outperforms methods based on first-order approximations. As discussed in the main paper, obtaining fully accurate hypergradients would require tracking and computing full Hessian matrix products, which is computationally prohibitive for diffusion models. Future work could explore more accurate yet efficient estimation strategies. Third, we acknowledge that when the downstream fine-tuning dataset is entirely composed of toxic data, both our method and existing baselines inevitably experience an increase in harmfulness. We believe that perfect resilience under such adversarial conditions is intrinsically difficult, given the strong generalization and few-shot capabilities of modern diffusion models. Nonetheless, our method demonstrates stronger resilience compared to baselines, maintaining relatively low IP even under fully toxic fine-tuning. Forth, similar to previous works, the NSFW classifiers used in our experiments are not perfectly accurate, and there might be false negatives or false positives. However, as all methods are evaluated under the same setting, the results are still fair and comparable to a large extent. We hope future work can build more accurate classification models. Finally, while we designed and evaluated adversarial & adaptive attacks and demonstrated ResAlign’s robustness against them, we recognize that stronger or more sophisticated attacks may emerge in the future. Developing robust defenses against such potential threats remains an important direction for future work.